IEEE Access
Multidisciplinary | Rapid Review | Open Access Journal

Received 22 December 2023, accepted 19 February 2024, date of publication 23 February 2024, date of current version 8 March 2024.

Digital Object Identifier 10.1109/ACCESS.2024.3369471

RESEARCH ARTICLE

Study on Stray Light Testing and Suppression Techniques for Large-Field of View Multispectral Space Optical Systems

YI LU[1], XIPING XU[1], NING ZHANG[1], YAOWEN LV[1], AND LIANG XU[2]

[1]National Demonstration Center for Experimental Opto-Electronic Engineering Education, School of Opto-Electronic Engineering, Changchun University of Science and Technology, Changchun 130022, China
[2]Xi'an Institute of Optics and Precision Mechanics of CAS, Xi'an 710119, China

Corresponding authors: Yi Lu (luyi@cust.edu.cn) and Xiping Xu (xxp@cust.edu.cn)

This work was supported in part by the Science and Technology Research Project of Education Department of Jilin Province, China, under Project JJKH20220753KJ; in part by the 111 Project of China under Grant 17017; and in part by the National Demonstration Center for Experimental Opto-Electronic Engineering Education.

ABSTRACT To evaluate the ability of space optical systems to suppress off-axis stray light, this paper proposes a stray light testing method for large-field of view, multispectral spatial optical systems based on point source transmittance (PST). And a stray light testing platform was developed using a high-brightness simulated light source, large-aperture off-axis reflective collimator, high-precision positioning mechanism and a double column tank to evaluate the stray light PST index of spatial optical system. On the basis of theoretical analyses, a set of calibration lenses and stray light elimination structures such as hoods, baffle and stop are designed for the accuracy calibration of stray light testing systems. The theoretical PST values of the calibration lens at different off-axis angles are analyzed by Trace Pro software simulation and compared with the measured values to calibrate the accuracy of the system. The testing results show that the PST measurement range of the system reaches 10^{-3} $\sim 10^{-10}$ when the off-axis angles of the calibration lens are in the range of $\pm 5^{\circ}$ $\sim$ $\pm 60^{\circ}$. The stray light test system has the advantages of wide working band, high automation and large dynamic range, and its test results can be used in the correction of lens hood and other applications.

INDEX TERMS Multi-spectrum, large-field view, stray light, point source transmittance (PST), lens hood.

I. INTRODUCTION

With the rapid development of space optics technology and the continuous improvement of the sensitivity of photoelectric detectors, the space optical systems with large field of view, multi-spectrum and high resolution are extensively used in aviation and aerospace [1]. The stray light suppression capability and evaluation index of the space optical system are becoming increasingly stringent [2]. Stray light usually refers to non-target, non-imaging light that reaches the image surface of an optical system through multiple refraction and reflection. It directly reduces the image contrast of the optical system and the signal-to-noise ratio of the detection target, and generates speckle spots on the image surface. In severe cases, the target signal will be completely annihilated in the noise of stray light radiation, resulting in system failure [3], [4]. Therefore, it is necessary to develop a stray light system to conduct strict stray light testing for space-based space optical systems to evaluate its stray light suppression ability.

Stray light can be categorized into the three types according to the sources [5], [6], [7]:

(1) The stray light outside the field of view for space cameras mainly comes from strong radiation sources such as sunlight, starlight, and terrestrial light, etc. It is a non-imaging

The associate editor coordinating the review of this manuscript and approving it for publication was Norbert Herencsar.

light source that reaches the image surface of the detector through multiple scattering, reflection, refraction and diffraction of the internal components of the system. Such stray light is widely present in various space optical systems and is the main source of stray light in the visible light band optical system.

(2) The stray light in the field of view is the imaging light caused by surface defects and contamination of optical elements and travels to the image surface of the detector in an abnormal path. Among them, the additional image formed by the light reflected by any two surfaces in the optical system near the image surface is called ghost image.

(3) Internal thermal radiation stray light is the thermal radiation generated by the internal components of the optical system, which mainly exists in the infrared optical system.

There are two methods for evaluating the capability of optical systems to suppress stray light, i.e., the surface source method (black spot method) and the point source transmittance (PST) method.

The black spot method was proposed by the German scientist Görtbay in the 1970s. In this method, a black spot and a white spot are placed in the central area of the extended field of view with uniform brightness, and the luminance ratio between the two is calculated, which is the stray light coefficient on the image surface of the system [8], [9], [10]. However, the black spot method cannot sufficiently expand the light source and the tends to introduce measurement errors, it is not suitable for measuring large aperture optical systems. It is generally used to measure camera lenses with small aperture and simple structure [11], [12].

The PST method was put forward by Breault [13], [14], [15] in the 1970s, which was used to measure the stray light suppression ability corresponding to different off-axis angles. Henceforth, many institutions conducted research on the analysis and detection of stray light in optical systems using PST method. A measuring device called Black Hole was developed in Utah State University based on PST principle with the test aperture of ϕ203 mm, its test band covers ultraviolet, visible light and infrared light, and the PST testing capacity is less than 10^{-9} orders of magnitude [16]. A stray light testing device was designed for the primary mirror in a vacuum tank in Breault Research Organization. The device adopted a large-aperture collimator to achieve the test caliber of ϕ300, the test band covers visible light and infrared light, and the PST testing ability is less than 10^{-5} magnitude of visible light and less than 10^{-6} magnitude of infrared light [17]. WANG Zhile et al set up a set of off-axis parabolic reflective measuring device with unobstructed center. The light source of the device is a high-voltage short-arc xenon lamp with a power of 10KW and a color temperature of 6000K. It is used to measure the Cassegrain telescope system with a diameter of ϕ300 mm, focal length of 1200 mm and a full field of view of 1.5°, and the PST measurement result is better than 10^{-6} orders of magnitude [18]. The three-band PST stray light testing device developed by ZHAO Jianke et al [19], has a testing aperture of 1m. The device uses a laser as light source, covering visible light, short wave infrared, and long wave infrared. The PST testing capability in the visible light band is less than 10^{-8}, and the infrared band is less than 10^{-6}. These testing devices have limitations for the tested optical system, such as aperture less thanϕ300 mm or PST testing threshold greater than 10^{-10}.

TABLE 1. The comparison of the ultimate testing capabilities of the point source transmittance testing system.

Test device	The maximum test aperture	Spectral band of light source	PST test capability
A measuring device called Black Hole	⌀203 mm	ultraviolet, visible light and infrared light	less than 10^{-9}
A stray light testing Device was designed for the primary mirror in a vacuum tank	⌀300 mm	visible light and infrared light	less than 10^{-5}
A set of off-axis parabolic reflective measuring device with unobstructed center	⌀300 mm	visible light	less than 10^{-6}
The three-band PST stray light testing device	⌀1000 mm	visible light, short wave infrared, and long wave infrared	less than 10^{-8}
The test device	⌀1000 mm	visible light and infrared light	less than 10^{-10}

This study focuses on developing a large field of view, multi-spectrum PST test device, and designing the calibration lens and stray light structure for system calibration. The maximum aperture of the measured optical system can reach ϕ1000 mm. The test band covers both visible and infrared light. The visible light PST testing ability is better than the 10^{-10} level, and the infrared PST testing capability is better than the 10^{-6} level. The test accuracy (test value/theoretical value) is better than 0.5. This device has good adaptability to large field of view and multispectral space optical systems. Table1 shows the comparisons of the ultimate testing capabilities of the point source transmittance testing systems.

II. WORKING PRINCIPLE OF STRAY LIGHT TEST SYSTEM

PST is a commonly used stray light evaluation standard, which represents the attenuation ability of optical-mechanical systems to stray light. PST is defined as [20]:

$$PST = \frac{E_{\mathrm{d}}(\theta)}{E_{\mathrm{i}}} \tag{1}$$

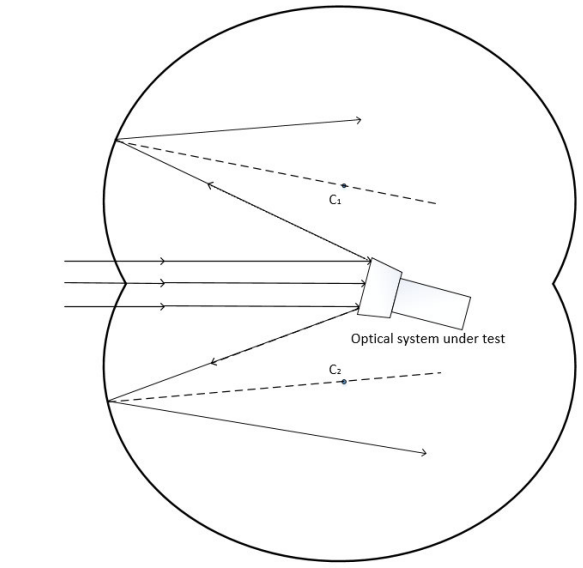

(a)

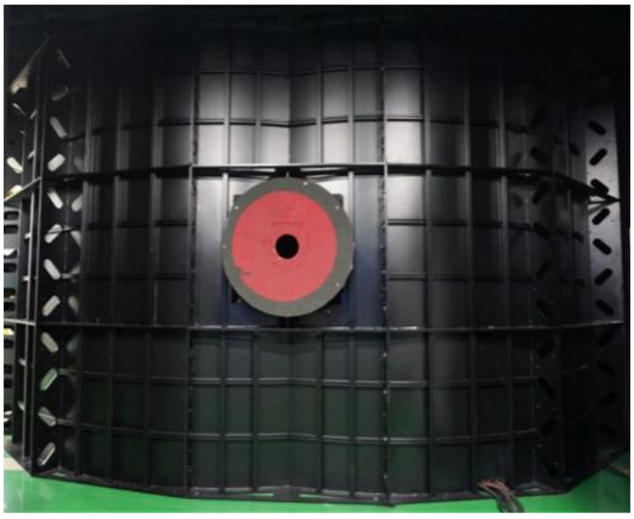

(b)

FIGURE 1. Double column tank based on point source transmittance test system: (a) An optical path analysis diagram of stray light from a double column tank structurel; (b) Physical drawing of double column tank.

where, $E_d(\theta)$ refers to the irradiance generated at the image surface by the point source target radiation of the optical system's off-axis field of view angle θ after passing through the optical system, and E_i is its irradiance at the inlet pupil of the optical system.

PST is not related to the intensity of stray light source radiation, but rather to the incident angle θ of the light and the operating wavelength λ of the system. Air scattering is one of the main factors affecting the accuracy of stray light testing. To avoid serious impact of air scattering on the accuracy of stray light testing, the ''Vacuum Test Chamber Stray Light Testing System'' and ''High Cleanliness Double Column Tank Testing System'' are mainly used for high-precision PST testing [21], [22]. The first system reduces the numbers of dust particles by vacuuming the test

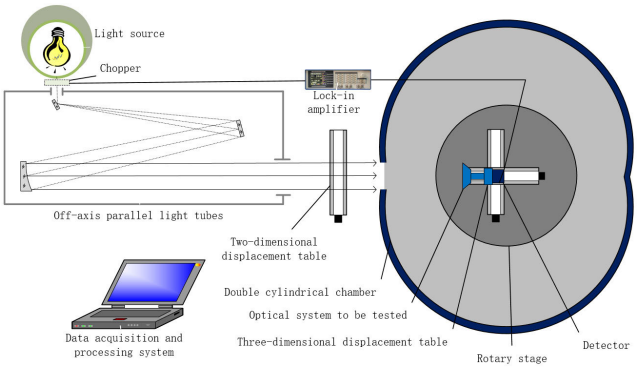

FIGURE 2. Schematic diagram of a large aperture and multi-spectral PST test system.

chamber, thereby effectively decreases Rayleigh scattering. However, the vacuum tank has limitations in sizes. Scattering from the inner wall increases if the size of the vacuum is too small, while larger sizes lead to high cost and difficulty in implementation. The second one adopts a large-sized testing chamber for double column tank, and the inner wall material is made of black acrylic plate with high absorption and low reflection, which effectively suppresses the inner reflection. The principle of eliminating stray light in the double column tank is ''absorption+ reflection'', shown in Figure1 [23], [24]. Most of the light entering the double column tank can be absorbed by the acrylic plate, and the unabsorbed light leaves the test light path in the form of mirror reflection, thus playing a dual role of ''removing stray light''. There are two different spherical centers C1 and C2 in the inner wall of the double column tank. The optical system to be measured is located between the two spherical centers. The two spherical centers of the double column tank do not coincide, the primary scattered light will not return to the measured optical system after being reflected by the inner wall, so it can play a role in eliminating stray light. The environmental cleanliness of the double column tank reaches the level of thousands, which greatly reduces Mie scattering, makes air scattering dominated by Rayleigh scattering, and improves the PST test accuracy of the system.

The system uses a black double column tank structure to test PST stray light. The simulation analysis shows that the stray light suppression of double-column tank can reach 10^{-10} orders of magnitude as the off-axis angle is greater than 50°. PST has high requirements for the space size and air cleanliness of the test system, but it has no requirements for the caliber of the tested system. The PST method has become an inevitable trend in the development of multi-spectral, large-diameter and high-precision stray light testing technology.

III. EXPERIMENTAL DEVICE FOR STRAY LIGHT TEST SYSTEM

According to the PST test requirements of multi-spectrum, large aperture, high precision and large dynamic range, a stray light test system is developed, as shown in Figure 2. The

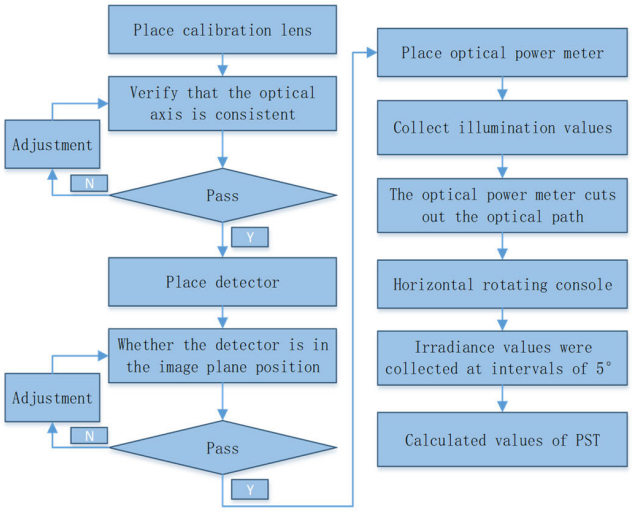

FIGURE 3. Experimental flow chart.

system consists of high brightness analog light source, large aperture off-axis reflective collimator, high precision positioning mechanism, detection system and high cleanliness double column tank test system.

The incident light is collimated by the collimator to form a uniform light spot of ϕ1000 mm, which enters the double column tank to fill the inlet pupil of the optical system to be measured.

The light energy detector is fixed on the two-dimensional scanning device placed at the exit of the collimator, to measure the irradiance E_i at the pupil of the measured optical system. After completing the measurement, the light path of the light detector will be cut off.

The chopper is located at the outlet of the light source and is used to periodically modulate the light source. The lock-in amplifier extracts the $E_d(\theta)$ of the PST signal from the low signal-to-noise ratio signal in terms of the frequency of the radiation light source.

The tested optical system is installed on an electronic control turntable, which can rotate to a fixed angle. The visible light detector (infrared detector) is mounted on a three-dimensional stage, which is adjusted to face the phase plane of the measured optical system.

The tested optical system can rotate around the Z-axis within $\pm 60°$ through revolving the electronic control turntable, to test the irradiance at different angles of the image plane.

The PST indices at different angles are calculated according to Eq. (1).

The calibration lens is used to measure the large aperture and high-precision PST test system. Therefore, the stray light suppression level of the calibration lens is obtained, and the PST measurement accuracy of this system is evaluated.

The specific experimental flow chart is as follows:

In order to improve the PST testing limit of the system, while maintaining the sensitivity of the detector, the higher the illuminance of the light source, the greater the light energy attenuated by the optical system on the detector, and the higher the signal-to-noise ratio on the photosensitive surface of the detector. Therefore, the testing limit and accuracy of the testing system PST can be adjusted higher.

This testing system uses a uniform polychromatic light source and five laser light sources with wavelengths of 0.447μm, 0.66 μm, 0.75 μm, 1.71 μm, and 2.2 μm, respectively. Light sources cover visible and infrared light bands. Uniform polychromatic light is used to simulate solar light sources, while laser light sources provide discrete band light sources.

The components of light source are fixed on a horizontal stage and can be freely switched. The light source is exported from the optical fiber and located at the focal plane of the collimator. In this paper, the calibration of the laser source with a spectrum of 0.66μm is analyzed and elaborated. Because the laser divergence angle after shaping is less than or equal to the aperture angle of the collimator, it can be considered that all the laser energy enters the collimator. According to the aperture and transmittance of the collimator, the illumination of the outgoing beam of the parallel optical tube can be obtained as follows:

$$E_i = \frac{Q}{S}\tau = \frac{1.2}{\pi(0.5)^2} \times 0.82\text{W/m}^2 = 1.25\text{W/m}^2 \quad (2)$$

where, Q is the output energy of the laser, S is the optical output area of the collimator, and τ is the optical efficiency of the system.

PST testing range of the system is between 10^{-3} ~10^{-10}. When the PST test magnitude is 10^{-10}, the lowest irradiance on the optical image plane can be calculated as:

$$\begin{aligned} E_{d1} &= \text{PST} \times E_i = 10^{-10} \times 1.25\text{W/m}^2 \\ &= 1.25 \times 10^{-10}\text{W/m}^2 \end{aligned} \quad (3)$$

When the PST magnitude is 10^{-3} tested, an attenuator with 1% transmittance should be installed in front of the detector. In this case, the irradiance on the optical image plane is:

$$\begin{aligned} E_{d2} &= \text{PST} \times E_i \times 0.01 = 10^{-3} \times 1.25 \times 0.01\text{W/m}^2 \\ &= 1.25 \times 10^{-5}\text{W/m}^2 \end{aligned} \quad (4)$$

The sensitivity range of the detector for visible light sources should be greater than 1.25×10^{-10}W/m^2 ~1.25×10^{-5}W/m^2. The main parameters of the three detectors in this paper are shown in Table 2.

IV. DESIGN OF CALIBRATION LENS AND STRUCTURE FOR ELIMINATING STRAY LIGHT

A. DESIGN OF CALIBRATION LENS

The optical design of the test system is closely related to the propagation of stray light. Stray light is mainly scattered and reflected by mirrors, and is transmitted through the optical system to finally reach the image surface. With satisfying the requirements of the design parameters, the number of optical surfaces should be minimized, the working distance of the optical system should be increased, and the position of the

TABLE 2. Main performance parameters of detector.

Detector type	Model	Spectral response range	Measuring range
Visible light detector	H9307-03	185nm-900nm	9.7×10^{-11} W/㎡- 3.1×10^{-4} W/㎡
Infrared light detector	IGA2.2-030-TE2-H	1.2μm-2.4μm	3.8×10^{-8} W/㎡- 6.37×10^{-3} W/㎡
Light energy detector	PM100USB	185nm-25μm	100 pW-200 W

TABLE 3. Summary of specific optical system indicators.

Serial number	Parameters of optical system	Design Results
1	Operating band（Central wavelength μm）	0.66
2	Focal length（mm）	250
3	angle of field（°）	6
4	F number	5

input pupil should be moved forward as far as possible. It also facilitates the modeling analysis of stray light at a later stage, and a calibration lens with a relatively simple structure is designed. The lens material is all H-ZF7LA, and the surface is coated with anti-reflection film. Its transmittance is greater than 97% in the visible band, and reaches 99% in the 0.66 μm band. Specific indicators are shown in Table 3. The optical structure is shown in Figure 4, and the design results are shown in Figures 5,6 and 7. The system meets the design requirements, has excellent imaging quality, and is easy to install and adjust the optical machine later.

B. ANALYSIS OF THE SURFACE RADIATION ENERGY TRANSFER MODEL

Stray light transmits part of its energy from one component surface to another by scattering and reflection, and there are emitting and receiving surfaces in the transmission process. Therefore, stray light is divided into a number of micro-surface elements with the same area, and the total sum of the radiation integral of the micro-surface elements arriving at the image surface is stray light arriving at the image surface [25], [26]. The radiative energy transfer is shown in Figure 8.

In Figure 8, dA_s represents the area element transmitting micro-bin, L_s represents its radiation brightness, dA_c represents the area element of receiving surface, θ_s the angle between the normal of the he area element of transmitting surface and the central line, and θ_c the angle between the normal of the area element of receiving surface and the central line. R_{sc} is the distance between the centers of two area elements.The radiation flux ($d\phi_c$) received by the receiving surface element (dA_c) from the transmitting surface element (dAs) is [27]:

$$d\phi_c = dA_s \cdot L_s \cdot \cos\theta_s \cdot \frac{dA_c \cdot \cos\theta_c}{R_{sc}^2} = \mathrm{BSDF} \cdot \mathrm{GCF} \cdot d\phi_s \tag{5}$$

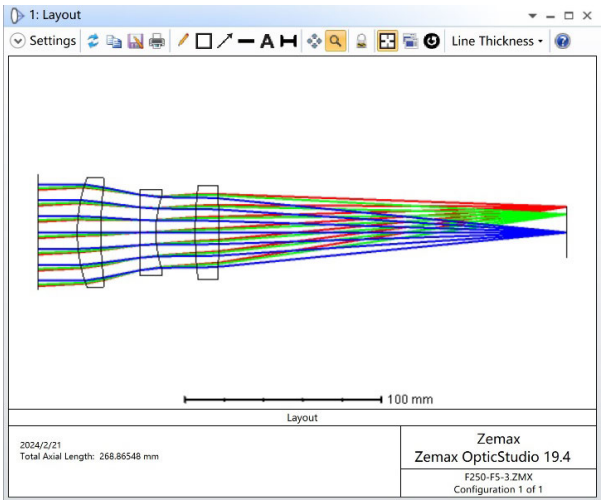

FIGURE 4. Structure diagram of the optical system.

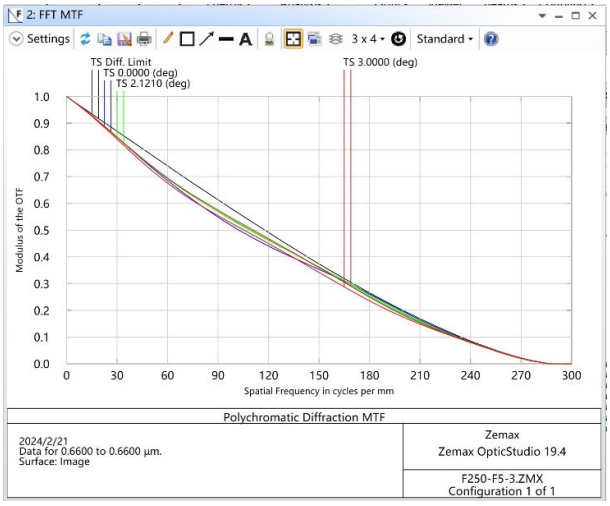

FIGURE 5. MTF curve of optical system.

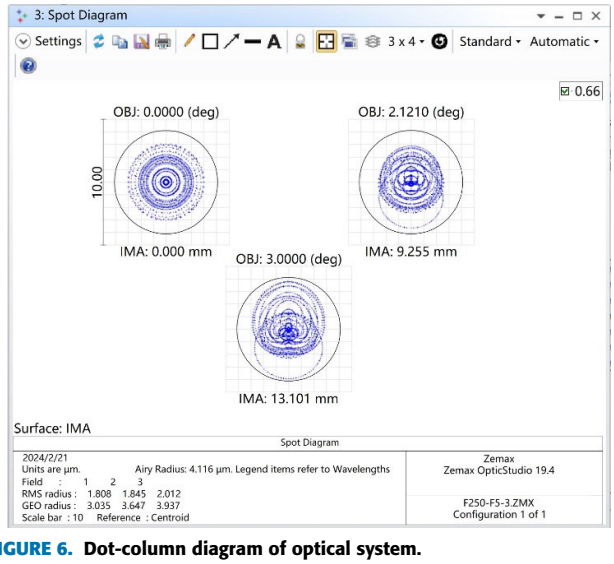

FIGURE 6. Dot-column diagram of optical system.

In Eq. (5), BSDF is the surface bidirectional scattering distribution function, GCF the geometric factor, and $d\phi_s$ the emitting surface radiation flux. It can be seen that it is

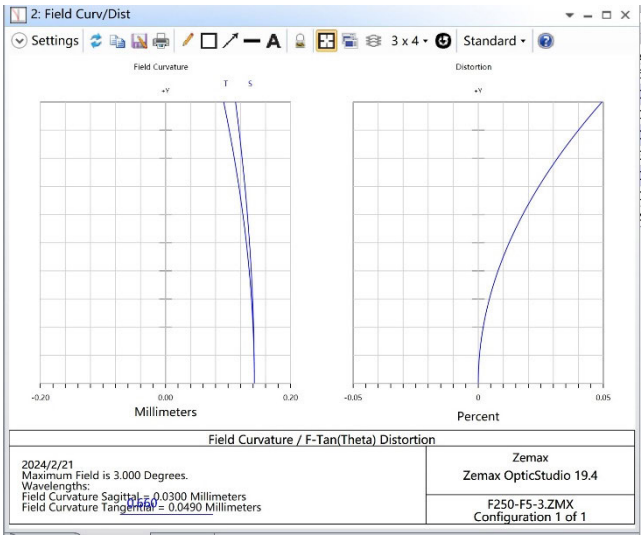

FIGURE 7. Field curvature and distortion diagram of optical system.

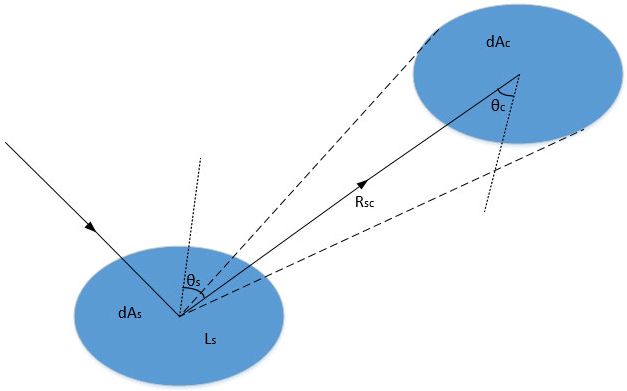

FIGURE 8. Schematic diagram of radiation energy transfer of stray light source.

necessary to reduce the radiation flux $d\phi_c$ of the receiving surface dA_c in order to suppress stray light, which can be achieved in the following three ways [28], [29], [30]:

(1) Reduce BSDF: treatment of the surface of the structural parts of the optical machine, such as surface blackening treatment of mechanical parts, surface coating treatment of optical parts, etc.

(2) Reduce GCF: reduce the geometric components of stray light transmission at each level, add light blocking structures to the system, such as hoods and diaphragms, etc.

(3) Reduce $d\phi_s$: reduce the radiation energy emitted from the upper surface, such as the use of filters, reduce the working temperature, etc.

C. DESIGN OF STRAY LIGHT ELIMINATION STRUCTURE

A light shield is used to restrict stray radiation outside the field of view from entering the optical system through a single reflection without obstructing the effective light within the field of view. The longer the hood is, the more conducive to blocking large angles of stray light radiation. However, it will increase the weight and volume of the system, and even

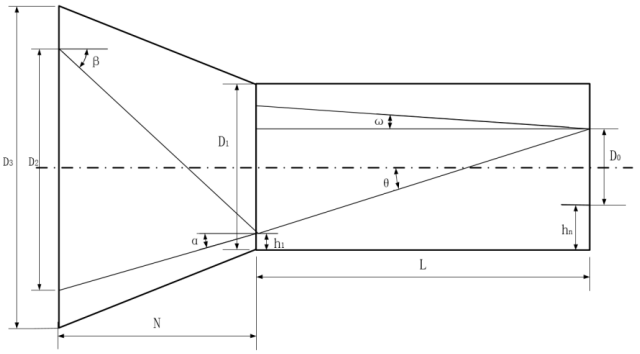

FIGURE 9. Schematic diagram of two-stage hoods.

hinder the propagation of edge optics [31], [32], [33]. The stray light sources of the space optical system are complex and may have multiple sources such as moonlight and terrestrial light at the same time [3]. Therefore, the structure of two-stage hoods is adopted in this experiment, as shown in Figure 9. The first stage is mainly used to suppress stray light from large angles outside the field of view, and the second stage is mainly used to suppress stray light from small angles. The two-stage hood structure effectively suppresses the influence of stray light.

In Figure 9, D_0 is diameter of the aperture and $D_1$is the outer diameter of the primary hood of the optical system, respectively. D_2 is the diameter of the inlet aperture of the secondary hood, D_3 is the outer diameter of the aperture of the secondary hood. h_1 is the height of the front baffle of the hood, h_n is the height of the rear baffle, θ is the avoidance angle of the test system, ω is the half-field angle of the optical system, α is the half-tension angle of the secondary hood, β is the suppression angle of the stray light source, L is the primary hood length, N is the length of the secondary hood. Then the total length S of the hood can be calculated according to Eq. (6), (7), (8) and (9). (The above length units are in millimeters.)

$$\tan\omega = \frac{h_n - h_1}{L} \tag{6}$$

$$D_1 = D_0 + 2h_n \tag{7}$$

$$L = (D_1 - h_1)\tan\theta + (D_0 + h_n)\tan\left(\frac{\pi}{2} - \theta\right) \tag{8}$$

$$N = \frac{d(\tan\omega + \tan\alpha)}{(\tan\beta - \tan\alpha)(\tan\alpha - \tan\omega)} \tag{9}$$

The total length S of the two-stage hoods is:

$$S = L + N \tag{10}$$

To further suppress stray light from entering the optical system, multiple gradient-arranged baffles are used inside the hood. When stray light is incident on the inner wall of the hood through the apex of the baffle, scattered light in any direction of the stray light cannot reach the input pupil of the optical system directly due to the baffle of the next baffle [34], [35], [36].The interaction between the inner wall of the hood and the baffle constitutes a semi-closed light trap, which

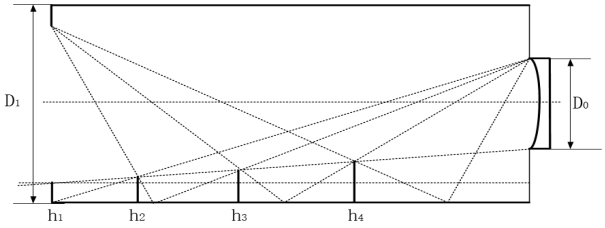

FIGURE 10. Structural diagram of cylindrical gradient arrangement baffle ring.

greatly increases the propagation path of stray light to the optical system, dissipates transmission energy many times, and has a good suppression effect on stray light from large off-axis angles. Its structure is shown in Figure 10.

When stray light enters the imaging system through the inside of the hood, the structure of the diaphragm can be reasonably set up inside the system to suppress stray light and achieve effective blocking or attenuation of stray light. Commonly used include aperture stops, field-of-view stops and Lyot stops, etc [37], [38], [39]. The aperture stop is used to control the size of the beam incident range in the optical system, and a reasonable setting of the aperture stop position in the optical system can effectively reduce the energy scattered by stray light on the detector [40], [41], [42]. In general, the closer the aperture stop is to the image plane, the better the stray light suppression capability. However, this also makes the rear of the aperture stop a ''critical surface'', i.e., a surface that reflects the incident stray light directly to the detector. The more ''critical surfaces'' the detector can see, the less conducive to suppressing stray light, which requires that the number of optical elements between the aperture stop and the detector be reduced as much as possible to avoid scattering and diffraction of stray light [43], [44].

Based on the principle that the optical system can correct aberration and the simple structure, the aperture stop of this system is optimized and placed on the left surface of the second lens, as shown in Figure 11, which can effectively suppress some stray light scattered in the front part of the system and achieve the best suppression effect. Also, the ''critical surface'' needs to be sprayed black or increase the surface roughness and other processes to ensure that its absorption rate is above 90%, which is conducive to reducing the illumination of stray light on the image surface [45], [46].

According to design requirements, the calibrated lens (including the hood) is processed and adjusted, and the adjusted effect is shown in Figure 12.

V. TEST RESULTS AND ANALYSIS

A. STRAY LIGHT TEST RESULTS

According to the design principle of the PST test system, a test platform is built, shown in Figure 13.

Using the calibration lens, the PST test of the hyperspectral space optical system with large field of view is carried out in the off-axis angle range of $\pm 5^\circ \sim \pm 60^\circ$. The specific test process is as follows.

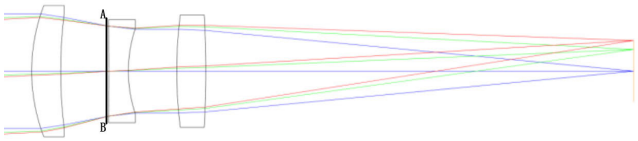

FIGURE 11. Diagram of the position of the aperture diaphragm set in the optical path.

FIGURE 12. Physical drawing of calibration lens (including hood) after installation and adjustment.

(1) Place the calibration lens on the electric control turntable, and its optical axis is consistent with that of incident light, and take this position as the reference position.

(2) Fix the detector on the three-dimensional displacement table and adjust the three- dimensional stage to maximize the optical power of the detector, so as to ensure that the detector is located in the image plane of the calibration lens.

(3) Fix the optical power meter on the two-dimensional scanning device, and the travel of the scanning device should cover the whole emergent light spot, so that the optical power meter can pass through the light spot in an S shape, and collect the illuminance values of 10 points, with the average value is the irradiance at the entrance pupil E_i.

(4) Cut the optical power meter out of the optical path, control the turntable to rotate horizontally to make it scan and record at intervals of 5° around the reference position, and then the irradiance at the image plane of the calibration lens is $E_d(\theta)$.

According to the design principle of the PST test system, the PST test of the large field of view and hyperspectral space optical system is carried out in the range of $\pm 5^\circ \sim \pm 60^\circ$ off-axis angle by using the calibration lens. To verify the stability of the system, the test was repeated three times. The test results are compared with the theoretical data, and the rationality of the design analysis is verified from the experimental results. The test curve is shown in Figure 14.

Figure. 14 shows the comparison of the data between the analytical and testing results. The test values are locally slightly larger than the design ones. This is mainly due to the measurement error introduced by excessive background noise caused by air scattering in the test environment. Improving cleanliness to 100 levels (ISO5 level) can effectively reduce this error. The suppression effect is obvious when the off-axis

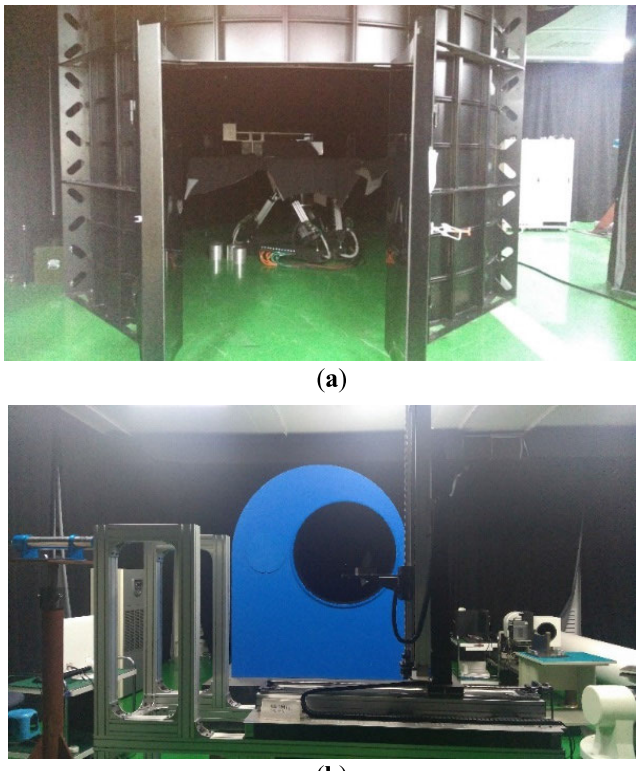

FIGURE 13. Physical diagram of test system: (a) Double column tank and internal electronic control turntable; (b) Collimator and two-dimensional stage.

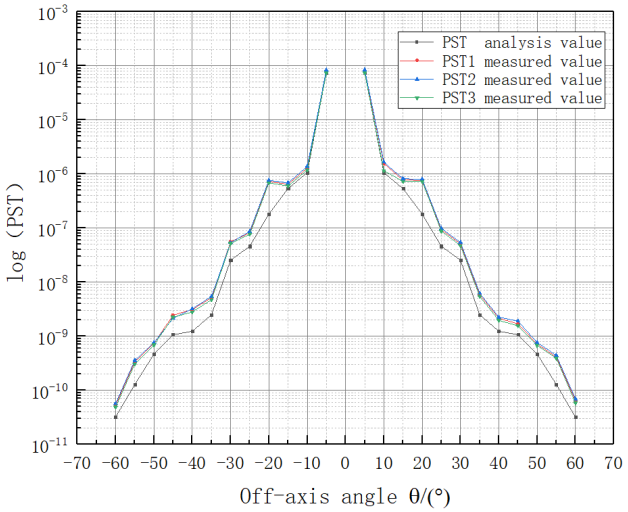

FIGURE 14. Comparison of PST analysis values and test values for calibration lens.

angle is between $\pm 5^{\circ} \sim \pm 10^{\circ}$. The PST value reaching 10^{-6} magnitude indicates that the system has significant effect to the suppression of stray light, and the experimental design is reasonable. When the off-axis angle is less than $\pm 15^{\circ}$, the test value of the calibration lens has a relatively stable agreement with the design one, and the PST value is better than 10^{-6} orders of magnitude. When the off-axis angle

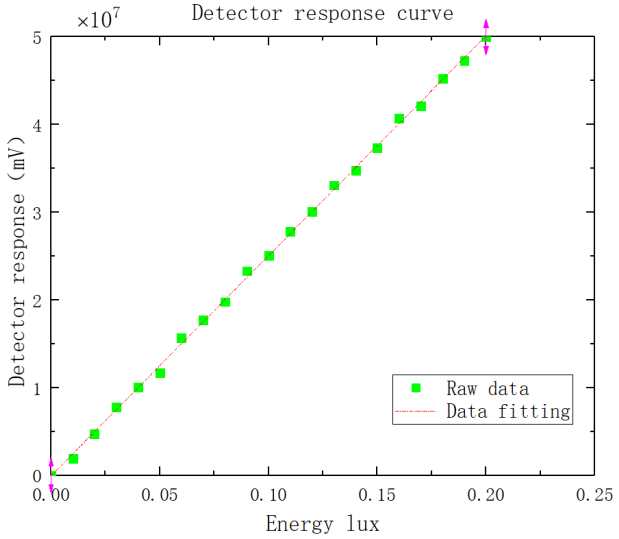

FIGURE 15. Detector response curve.

is greater than $\pm 15^{\circ}$, the test value is slightly larger than the design one. This is because when the system tests the PST value at a large angle, a large amount of stray light is reflected and scattered into the measured optical system in the double column tank, making the measurement result large and increasing with the off-axis angle. There is a big difference in the values around $\pm 20^{\circ}$, which may be due to the analysis error of the surface attribute model of the hood, or the error generated in the process of system processing and assembly. These errors also contribute to the incomplete symmetry of the test curve. When the off-axis angle is $\pm 60^{\circ}$, the PST test value is better than 10^{-10} orders of magnitude. On the whole, the actual measurement results are basically consistent with the theoretical design values and fully satisfy the design and calibration requirements.

B. ERROR ANALYSIS OF TEST RESULTS

The PST measurement errors in the test system mainly include systematic and random errors. Systematic errors mainly include the structure and surface scattering errors of the double column tank and the errors caused by air cleanliness, which affect the limit value of the PST test. Random errors mainly include errors caused by the stability of the light source and the linearity of the detector, which affect the measurement accuracy of the test data.

The effect of the double-column tank structure to the PST test limit value is mainly caused by the mirror image return of the scattered light when the off-axis angle is large. When the off-axis Angle is small, the reflected light will not return the original way due to the unique structure that the two centers of the two-column tank are not concentric. When the off-axis Angle is increased (greater than $\pm 60^{\circ}$), the off-axis angle of the photometric system tends to be collinear with the center of the two circles, therefore, the diameter of the double-column tank can be increased to ensure the stray light suppression effect. When the off-axis angle approaches to

±90°, the error caused by the two-column tank structure cannot be eliminated, and such cases should be avoided. At the same time, the inner wall and air cleanliness of the double column tank will also affect the test limit of PST. The cleanliness of the environment in this experiment has reached the level of 1000, which has little effect on the experimental results.

The detector is suitable for weak signal detection at large off-axis angle, and the dynamic range is up to 10^7. The detector response curve is shown in Figure 15. The nonlinear error is ±5%, and the stability of the light source is 1.2%/100min after the experiment. Therefore, errors due to detector linearity and source stability are:

$$\Delta = \sqrt{(5\%)^2 + (1.2\%)^2} = 5.1\% \tag{11}$$

VI. CONCLUSION

The measurement of stray light is significant to determining and verifying the ability of space optical system to suppress stray light. This paper provides a feasible measurement scheme. This study fully proves that the point source transmittance method is more suitable for space optical systems with large aperture and high stray light suppression ratio. The experimental results show that the PST measurement range of the system reaches 10^{-3} ~10^{-10}, which fully meets the test requirements, and provides a reference for the suppression of stray light in space optical systems. The specific research results are as follows:

(1) By analyzing the energy transfer model of surface radiation, stray light can be suppressed from three aspects, among which the design of hood, halo and aperture is the most direct and effective method to suppress stray light from reaching the detector.

(2) A calibration lens is designed, which can calibrate the precision of large-aperture and high-precision PST test system. Through the analysis and comparison between the measured data and the design values, the system measurement ability can be verified, and the calibration problem of high-precision PST test system can be solved.

(3) The anti-stray light structure is designed. The design of two-stage hood can greatly reduce the influence of off-axis stray light with large field of view, and the internal light baffle can ensure that the primary scattered light cannot directly irradiate the interior of the optical system after the external light source irradiates the inner wall.

(4) The theoretical value of PST for calibrating the lens system is simulated and analyzed by TracePro software. Finally, the test accuracy of the calibration lens, that is, the calibration error of the test system, is obtained by comparing the measured value with the theoretical value. The experimental results show that the calibration error is better than lg/0.5, which completely meets the requirements of the test system.

In the future, with the continuous maturity of theory and practice, the stray light testing and suppression technology of large-field multi-spectral spatial optical system will be further improved in the following three aspects.

(1) Improve the test limit and test accuracy of large-caliber and high-precision PST system;

(2) Strengthen the research on stray light testing technology of infrared spectrum and improve the PST testing ability of infrared system;

(3) The stray light test and simulation are combined to accurately guide the optimal design of optical system.

Efficient stray light suppression and precision evaluation technologies support the development of future space optical systems for many applications, such as very large field of view, multispectral, and faint targets. With the development and improvement of stray light suppression and evaluation technology, scientific research fields such as space astronomical optical observation can be better guaranteed.

REFERENCES

[1] W. Sutherland et al., "The visible and infrared survey telescope for astronomy (VISTA): Design, technical overview, and performance," *Astron. Astrophys.*, vol. 575, p. A25, Mar. 2015.

[2] D. Frostig, J. Piotrowski, K. Clark, D. Coppeta, M. Egan, G. Fżrész, M. Gabutti, R. Masterson, A. Malonis, and R. A. Simcoe, "Stray light analysis and reduction for IFU spectrograph LLAMAS," *Proc. SPIE*, vol. 11447, pp. 1446–1454, Dec. 2020.

[3] M. Montanaro, A. Gerace, A. Lunsford, and D. Reuter, "Stray light artifacts in imagery from the Landsat 8 thermal infrared sensor," *Remote Sens.*, vol. 6, no. 11, pp. 10435–10456, Oct. 2014.

[4] G. L. Peterson and M. Cote, "Lessons learned from the stray light analysis of the XMM telescope," *Proc. SPIE*, vol. 3113, pp. 321–333, Jun. 2014.

[5] J. Tian, X. Li, L. Hou, and Z. Xu, "Analysis and suppression of stray radiation in an infrared telescope system in geosynchronous orbit," *Proc. SPIE*, vol. 11548, Oct. 2020, Art. no. 115480I.

[6] D. Zhou and X. Wang, "Stray light suppression of wide-field surveillance in complicated situations," *IEEE Access*, vol. 11, pp. 2424–2432, 2023, doi: 10.1109/ACCESS.2023.3234052. https://doi.org/10.1109/ACCESS.2023.3234052

[7] H. Yuan, H. Zhang, and M. Sun, "Suppression of diffraction stray light in the inner-occulted coronagraph," *Scientia Sinica Technologica*, vol. 49, no. 11, pp. 1343–1349, 2019.

[8] Y. Zhao, Y. Xu, C. Chen, F. Zhang, and J. Ren, "Optical design and stray light analysis of the space infrared optical system," *J. Harbin Inst. Technol.*, vol. 24, no. 1, pp. 32–36, 2017.

[9] S. Mingzhe, H. Hongxin, L. Zhenwu, B. Heyang, M. Junlin, and W. Xiaoxun, "Stray light suppression of the large field of view coronagraph optical system," *Laser Optoelectron. Prog.*, vol. 51, no. 5, 2014, Art. no. 052203.

[10] S. Yijun and X. Ziqi, "Optical system design of star sensor and stray light suppression technology," *Infr. Laser Eng.*, vol. 50, no. 9, 2021, Art. no. 20210015.

[11] L. Qiang, "Study on stray light analysis and application technology of the Earth synchronous orbit space camera," Univ. Chin. Acad. Sci., Shanghai Inst. Tech. Phys., Shanghai, China, Tech. Rep., 2016, pp. 1–11.

[12] X. Zhong, Z. Su, G. Zhang, Z. Chen, Y. Meng, D. Li, and Y. Liu, "Analysis and reduction of solar stray light in the nighttime imaging camera of Luojia-1 satellite," *Sensors*, vol. 19, no. 5, p. 1130, 2019.

[13] X. Shao, X. Wu, F. Yu, and C. Cao, "Characterization and monitoring of GOES-16 ABI stray light and comparison with Himawari-8 AHI and GOES-17 ABI," *J. Appl. Remote Sens.*, vol. 15, no. 1, Feb. 2021, Art. no. 017503.

[14] T. Sun, F. Xing, J. Bao, S. Ji, and J. Li, "Suppression of stray light based on energy information mining," *Appl. Opt.*, vol. 57, no. 31, pp. 9239–9245, 2018.

[15] J. Li, Y. Yang, X. Qu, and C. Jiang, "Stray light analysis and elimination of an optical system based on the structural optimization design of an airborne camera," *Appl. Sci.*, vol. 12, no. 4, p. 1935, Feb. 2022, doi: 10.3390/app12041935.

[16] L. Zhaohui, Z. Jianke, X. Liang, L. Feng, G. Yi, L. Kai, and Z. Qing, "Precision calibration and analysis of point source transmittance measurement system," *Acta Physica Sinica*, vol. 65, no. 11, pp. 150–156, 2016.
[17] X. Liang, "Research on key technologies of stray light measurement for large aperture optical system," Univ. Chin. Acad. Sci., Xi'an Inst. Opt. Precis. Mech., Xi'an, China, Tech. Rep., 2019, pp. 5–9.
[18] W. Zhile, G. Zhongqiang, Z. Wei, and W. Fugang, "Measurement of stray light based on point-source transmittance in space optical system," *Optical Technique Papers*, vol. 37, no. 4, pp. 401–405, 2011.
[19] W. Hu, C. Qinfang, M. Zhanpeng, Y. Haoyu, L. Shangmin, and X. Yaoke, "Development and prospect of stray light suppression and evaluation technology invited," *Acta Photonica Sinica*, vol. 51, no. 7, 2022, Art. no. 0751406.
[20] H. Jiang and X. Niu, "Stray light analysis and suppression of the visible to terahertz integrated cloud detection optical system," *Sensors*, vol. 23, no. 8, p. 4115, Apr. 2023, doi: 10.3390/s23084115.
[21] X. Liang, G. Li-Min, Z. Jian-Ke, L. Feng, Z. Yan, L. Zhao-Hui, Y. Fei, and Z. Qing, "Calibration of stray light based on point source transmittance measurement system," *Opt. Precis. Eng.*, vol. 24, no. 7, pp. 1607–1614, 2016.
[22] V. Khodnevych, M. Lintz, N. Dinu-Jaeger, and N. Christensen, "Stray light estimates due to micrometeoroid damage in space optics, application to the LISA telescope," *J. Astronomical Telescopes, Instrum., Syst.*, vol. 6, no. 04, Dec. 2020, Art. no. 048005.
[23] H. Tang, J. Xie, X. Tang, W. Chen, and Q. Li, "On-orbit radiometric performance of GF-7 satellite multispectral imagery," *Remote Sens.*, vol. 14, no. 4, p. 886, Feb. 2022.
[24] L. Bo, F. Rui, K. Wei, and L. Wei-qi, "Optical system design and stray light suppression of catadioptric space camera," *Chin. Opt.*, vol. 13, no. 4, pp. 822–831, 2020.
[25] T. Hallberg, D. A. Pearce, P. Raven, C. J. Baker, R. P. Moore, and H. Kariis, "Round Robin comparison of BRDF measurements," *Proc. SPIE*, vol. 11158, Oct. 2019, Art. no. 111580I.
[26] Z. Jiao, A. Ding, A. Kokhanovsky, C. Schaaf, F.-M. Bréon, Y. Dong, Z. Wang, Y. Liu, X. Zhang, S. Yin, L. Cui, L. Mei, and Y. Chang, "Development of a snow kernel to better model the anisotropic reflectance of pure snow in a kernel-driven BRDF model framework," *Remote Sens. Environ.*, vol. 221, pp. 198–209, Feb. 2019.
[27] T. Arts, D. Tomuta, and V. Kirschner, "Black coatings BSDF database," *Proc. SPIE*, vol. 11852, Jun. 2021, Art. no. 1185261.
[28] L. Doyle, P. Khademi, P. Hilz, A. Sävert, G. Schäfer, J. Schreiber, and M. Zepf, "Experimental estimates of the photon background in a potential light-by-light scattering study," *New J. Phys.*, vol. 24, no. 2, Feb. 2022, Art. no. 025003.
[29] J.-Y. Xue, Y.-H. Cao, Z.-S. Wu, J. Chen, Y.-H. Li, G. Zhang, K. Yang, and R.-T. Gao, "Multiple scattering and modeling of laser in fog," *Chin. Phys. B*, vol. 30, no. 6, Jun. 2021, Art. no. 064206.
[30] C. Xing, H. Chun-Hui, Y. Chang-Xiang, and K. De-cheng, "Analysis and suppression of space stray light of visible cameras with wide field of view," *Chin. Opt.*, vol. 12, no. 3, pp. 678–685, 2019.
[31] Z. Tong, M. Li, C. Cui, Z. Huo, and B. Luo, "Design and analysis of the configuration of deployable membrane sunshield," *Chin. Space Sci. Technol.*, vol. 41, no. 3, pp. 82–88, 2021.
[32] Z. Xu, D. Liu, C. Yan, and C. Hu, "Stray light elimination method based on recursion multi-scale gray-scale morphology for wide-field surveillance," *IEEE Access*, vol. 9, pp. 16928–16936, 2021.
[33] L. Clermont and L. Aballea, "Stray light control and analysis for an off-axis three-mirror anastigmat telescope," *Opt. Eng.*, vol. 60, no. 5, May 2021, Art. no. 055106.
[34] C.-C. Wang, L.-M. Wei, X. Tian, L. Zhang, and Y. Xie, "New baffle design and analysis of long-wave infrared camera," *Optik*, vol. 242, Sep. 2021, Art. no. 166820.
[35] G. Wang, F. Xing, M. Wei, and Z. You, "Rapid optimization method of the strong stray light elimination for extremely weak light signal detection," *Opt. Exp.*, vol. 25, no. 21, p. 26175, 2017.
[36] L. Wei, L. Yang, Y.-P. Fan, S.-S. Cong, and Y.-S. Wang, "Research on stray-light suppression method for large off-axis three-mirror anastigmatic space camera," *Sensors*, vol. 22, no. 13, p. 4772, Jun. 2022, doi: 10.3390/s22134772.
[37] A. Hammar, O. M. Christensen, W. Park, S. Pak, A. Emrich, and J. Stake, "Stray light suppression of a compact off-axis telescope for a satellite-borne instrument for atmospheric research," *Proc. SPIE*, vol. 10815, Nov. 2018, Art. no. 108150F.
[38] P. Sandri, S. Fineschi, M. Romoli, M. Taccola, F. Landini, V. Da Deppo, G. Naletto, D. Morea, D. P. Naughton, and E. Antonucci, "Stray-light analyses of the multielement telescope for imaging and spectroscopy coronagraph on solar orbiter," *Opt. Eng.*, vol. 57, no. 1, 2018, Art. no. 015108.
[39] Z. Ma, Q. Chen, and H. Wang, "Simulation and analysis of atmospheric scattering in stray light testing for point source transmittance," *Appl. Opt.*, vol. 60, no. 2, pp. 232–238, Jan. 2021.
[40] H. Zhenqiang, L. Jian, S. Xiaozheng, L. Wei, L. Guoping, R. Qilong, and X. Yuanjing, "Joint design of light shield and satellite attitude control for GEO super large aperture camera," *Aerosp. Control Appl.*, vol. 48, no. 1, pp. 16–22, 2022.
[41] S. Chen and X. Niu, "Analysis and suppression design of stray light pollution in a spectral imager loaded on a polar-orbiting satellite," *Sensors*, vol. 23, no. 17, p. 7625, Sep. 2023, doi: 10.3390/s23177625.
[42] X. Li, X. Li, D. Li, X. He, and M. Jendryke, "A preliminary investigation of Luojia-1 night-time light imagery," *Remote Sens. Lett.*, vol. 10, no. 6, pp. 526–535, Jun. 2019.
[43] Y. Tao, L. Chunlin, and M. Qingliang, "Application of reflective ellipsoid grating system in space optical remotesensor," *Spacecraft Recovery Remote Sens.*, vol. 37, no. 2, pp. 74–81, 2016.
[44] J. Shouwang, X. Zhentao, S. Yongxue, and W. Ke, "Optical design and stray-light analysis of urban night-light remote sensing imaging system," *Laser Optoelectronics Prog.*, vol. 57, no. 1, 2020, Art. no. 012201.
[45] (Apr. 18, 2022). *Le Specialiste De La Finition Thermique Pour Satellites et Lanceurs: Conception, fabrication et Application De Revetements De Finition Thermique a Fort Heritage Technologique*. [Online]. Available: www.map-coatings.com
[46] Y. Z. Tuleushev, V. N. Volodin, E. A. Zhakanbaev, E. E. Suslov, and A. S. Kerimshe, "Fabrication of porous tantalum and tungsten black coatings for artificial Earth satellites," *Tech. Phys. Lett.*, vol. 46, no. 4, pp. 319–322, Apr. 2020.

YI LU received the M.Eng. degree in instrument science and technology from Changchun University of Science and Technology, in 2013, where he is currently pursuing the Ph.D. degree with the School of Optoelectronic Engineering.

He taught undergraduate students experimental courses in "Optical Instrument Design and Assembly Technology" and "Digital Image Processing." He guided students to a second provincial and ministerial award in competitions and was an Excellent Instructor. He has published more than ten articles in core journals. Over the past five years, he has chaired or participated in five national projects. His main research interests include optoelectronic inspection technology and quality control, optical instrument assembly, and adjustment.

Mr. Lu is a member of the China Instrument Association and China Optical Society.

XIPING XU received the Ph.D. degree in optical engineering from Changchun University of Science and Technology, in 2004.

He is currently the Executive Vice President of the Graduate School, Changchun University of Science and Technology. He is also a Professor and a Doctoral Supervisor. His main research interests include optical detection technology and quality control, with special features and advantages in the research of optical non-contact detection and quality control of geometry and form error, modern optical sensing technology and systems, and satellite control system component testing and calibration technology. As the Project Leader or a main Participant, he was awarded the ''Eighth Five-Year Plan,'' ''9th Five-Year Plan,'' ''National 863,'' ''National Natural Science Foundation of China,'' ''National Aerospace Research Center,'' ''National Natural Science Foundation of China,'' ''National Aerospace Research Center,'' and ''National Aerospace Research Center.'' He has more than 50 scientific research achievements, including the National Natural Science Foundation of China (NSFC) and the Ministry of Space, have been obtained, and more than 20 of them have reached the international advanced level by experts. He has published more than 70 academic articles in major journals at home and abroad, 37 of which are indexed by SCI and EI. The first author published a monograph ''Photoelectric dimensional inspection technology and application.''

Dr. Xu is also a member of the Teaching Steering Committee of Instrumentation in Higher Education Institutions of the Ministry of Education of China, from 2018 to 2022, the Deputy Director of the Teaching Committee of Instrumentation Science and Technology of China Mechanical Industry Education Association, the Executive Director of the Eighth Council of the Laboratory Instrumentation Branch of China Instrument Association, and the Deputy Director of the Optoelectromechanical Integration Technology Branch of China Instrument Society.

NING ZHANG received the Ph.D. degree in instrumentation science and technology from Changchun University of Science and Technology, in 2013.

She was named as an Associate Professor, in 2015, and a Professor, in 2022. As the project leader or a principal researcher, she has carried out research on high-resolution surround-view 360° video image sensing technology, refractive panoramic camera calibration technology research, transparent material thickness complex color confocal photoelectric detection technology research, target generator, high-resolution hyperspectral imager, laser distance detector, and small spectrometer. In the past five years, she has conducted 13 scientific research projects as the leader or the second leader, of which she has led and chaired one national scientific research project and two provincial A-class scientific research projects. She received One Jilin Provincial Science and Technology Progress Award. She has published more than 30 articles, including more than ten SCI and EI articles. Her main research interests include optoelectronic detection technology and quality control.

YAOWEN LV received the degree in electronic science and technology from Shaanxi University of Science and Technology, in 2009, and the Ph.D. degree from Changchun Institute of Optics and Precision Machinery Physics, Chinese Academy of Sciences, in 2014.

He has presided over One Project of General Armament of the People's Liberation Army, One Project of National Youth Fund, One Project of Excellent Young Talents of Jilin Province, Three Horizontal Projects, and Accumulated Scientific Research of nearly three million RMB in the past five years; and applied for one national invention patent. He has published more than 20 academic articles as the first author or corresponding author, including five SCI-retrieved articles and five EI-retrieved articles. His main research interests include optoelectronic detection and quality control, visual measurement, machine vision, and deep learning.

Dr. Lv is also a Reviewer of *Applied Optics*, *JOSA* journal, and *Journal of the Optical Society of America*.

LIANG XU received the Ph.D. degree in optoelectronic engineering from the University of Chinese Academy of Sciences.

He is currently a Senior Engineer with the Xi'an Institute of Optics and Precision Mechanics of CAS. He is also an external Doctoral Supervisor with the Changchun University of Science and Technology. He is mainly engaged in optical design and test technology research, based on modern optoelectronic measurement technology, and has proposed a variety of innovative optoelectronic measurement methods. He has been responsible for more than 50 major national pre-research projects and model tasks, published 14 articles, granted 44 patents, and won four provincial and ministerial awards.

Dr. Xu is a member of the First Young Expert Committee of Advanced Optical Manufacturing of Chinese Optical Engineering Society.